Macromolecules
ARTICLE

Macromolecules **2009**, *42*, 4845–4852 **4845**
DOI: 10.1021/ma900665v

Photoresponsive Nanogels Based on Photocontrollable Cross-Links

Jie He, Xia Tong, and Yue Zhao*

Département de chimie, Université de Sherbrooke, Sherbrooke, Québec, Canada J1K 2R1

Received March 27, 2009; Revised Manuscript Received April 30, 2009

ABSTRACT: We present a new and general strategy for preparing photoresponsive nanogels. It is based on using light to reversibly change the cross-linking density of nanogel particles to control their swelling degree in aqueous solution. This control mechanism allows for gradual volume change of nanogel particles by light. For proof of concept, diblock copolymers composed of poly(ethylene oxide) and poly[2-(2-methoxyethoxy) ethyl methacrylate-*co*-4-methyl-[7-(methacryloyl)oxyethyloxy]coumarin] (PEO-*b*-P(MEOMA-*co*-CMA)) were synthesized; nanogels could easily be prepared by first photo-cross-linking the micellar aggregates at $T >$ LCST of the P(MEOMA-*co*-CMA) block through dimerization of coumarin side groups upon absorption of $\lambda > 310$ nm UV light and then cooling the solution to $T <$ LCST to obtain cross-linked water-soluble polymer nanoparticles. Under $\lambda < 260$ nm UV light, the reverse photocleavage of cyclobutane rings could be used to reduce the cross-linking density, leading to the swelling of nanogel particles with a volume increase by about 90%. The reversibility of the photoinduced volume change, the effects of the molecular weight of P(MEOMA-*co*-CMA) block and the content of coumarin groups on the photoresponsive behavior, and the use of nanogel particles for photocontrolled release were investigated.

1. Introduction

Micro- or nanogels are usually hydrogels in the form of micro- or nanoscale particles that may have a faster reaction time to stimuli such as pH or temperature change as compared to bulk hydrogels.[1−5] With respect to pH- or thermosensitive systems there have been relatively few reports on microgels designed to respond to light.[6−10] The main approaches known for preparing photoresponsive microgels follow the strategies developed with bulk hydrogels.[11−14] One method consists in incorporating either chromophore molecules or nanoparticles in the microgel, whose absorption of light generates heat and induces the volume transition by elevating the temperature to above the lower critical solution temperature (LCST) of the polymer, being most often poly(*N*-isopropylacrylamide) (PNIPAM).[6−8] With the other method, microgels of random copolymers bearing spiropyran moieties were shown to be photoresponsive due to the photoisomerization between hydrophobic spiropyran and hydrophilic merocyanine.[9,10] Indeed, the photoinduced change in hydrophilicity could affect the LCST of the polymer and thus result in microgel's volume change at temperatures close to LCST.[10] A specific challenge in developing light-responsive microgels is how to achieve a gradual or graded volume change upon illumination, which is required for some particular applications. For instance, using the volume transition of a PNIPAM-based hydrogel induced by photothermal effect, Sershen et al. demonstrated a light-controllable valve that could either stop or allow the flow of a liquid in a microfluidic device.[15] It is conceivable that if the volume change of a photosensitive hydrogel can be graded, light can then be used to control the opening of the valve to tune the flow rate, instead of having only the closing and open states. Such a gradual volume change by light cannot be accomplished by means of the two known mechanisms.[6−15] On the one hand, with the thermal effect generated by light, the volume transition of PNIPAM occurs sharply at around its LCST (~32 °C) while it is difficult to fine-tune the solution temperature by controlling the amount of heat. On the other hand, the use of the spiropyran−merocyanine photoisomerization resulted in a small volume change effect,[10] and the effect is unlikely to be repeatable due to the easy degradation of the dyes. In the present study, we have investigated a general strategy to address the problem. Using nanogel particles (tens of nanometers in diameter) prepared from block copolymers self-assembly in aqueous solution, we demonstrate that light-induced gradual volume change is achievable based on a photocontrollable cross-linking density of the gel. This new control mechanism, which obviously can be scaled up and applied to larger size hydrogel particles, offers possibilities of developing more sophisticated photocontrollable hydrogels.

The design of such photoresponsive nanogels is schematically illustrated in Figure 1. It combines the use of block copolymer self-assembly and a reversible photo-cross-linking reaction. Basically, with a water-soluble diblock copolymer, one block of which displays a LCST and bears photochromic side groups, micelles can be obtained by heating the solution to $T >$ LCST and cross-linked by the photoreaction of the chromophore upon illumination at λ_1. By cooling the solution to $T <$ LCST, the preparation of nanogel is completed with cross-linked water-soluble nanoparticles. Because of the reversibility of the photoreaction, the cross-linking degree of the nanogel can be reduced in a controlled fashion by illumination at λ_2, which leads to swelling of nanogel particles. The initial cross-linking state can be recovered by recross-linking at $T >$ LCST. To validate the design, a series of diblock copolymers with the structure in Figure 1b were synthesized. They are composed of a block of poly(ethylene oxide) and a block of poly(2-(2-methoxyethoxy)ethyl methacrylate-*co*-4-methyl-(7-(methacryloyl)oxyethyloxy)coumarin), denoted as PEO-*b*-P(MEOMA-*co*-CMA) hereafter. The required reversible photo-cross-linking reaction is provided by the photodimerization of coumarin side groups under irradiation at $\lambda >$ 310 nm and the photocleavage of cyclobutane bridges under irradiation at $\lambda < 260$ nm.[16−18] As demonstrated by the present proof-of-concept study, optically controlling the cross-linking degree of nanogel particles could allow the control of the

*Corresponding author: e-mail yue.zhao@usherbrooke.ca.

Published on Web 05/18/2009

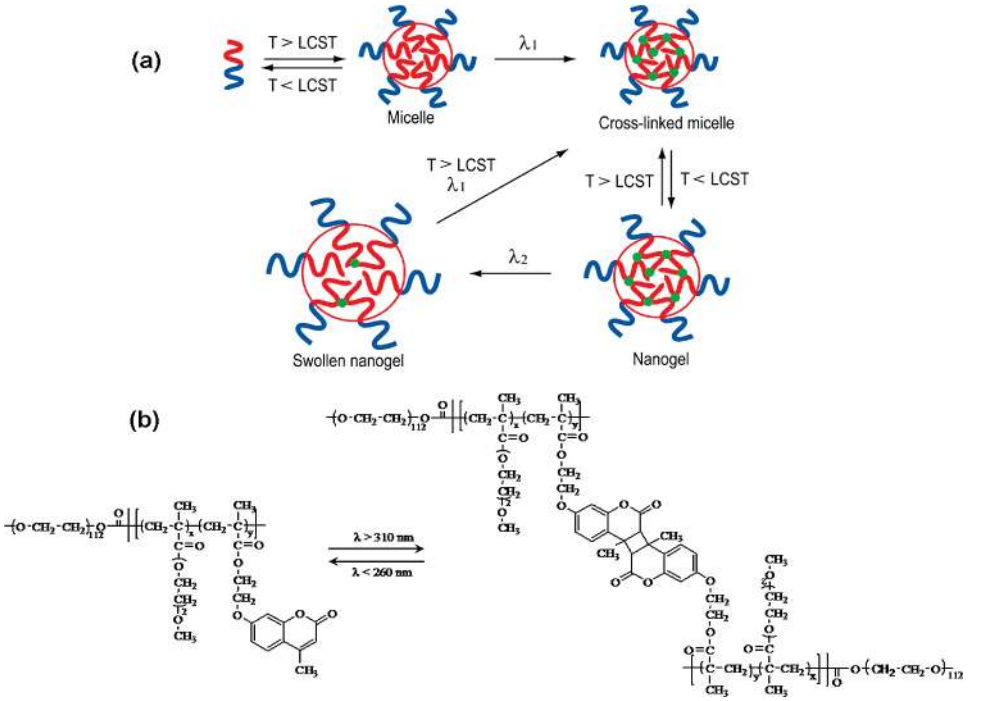

Figure 1. (a) Schematic illustration of the preparation and photocontrolled volume change of nanogel. (b) Designed diblock block copolymer bearing coumarin side groups for the reversible photo-cross-linking reaction.

Scheme 1. Synthetic Route to Diblock Copolymer PEO-*b*-P(MEOMA-*co*-CMA)

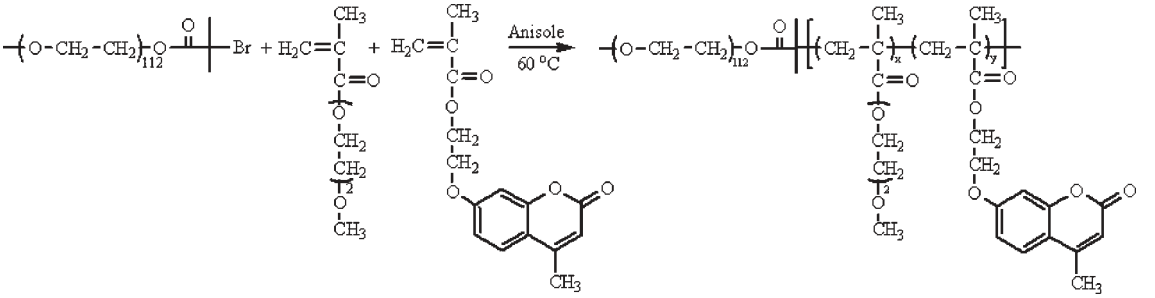

particles' volume change. We mention that PNIPAM nanogels prepared by using photo-cross-linking as well as thermosensitive block copolymer micelles photo-cross-linked at $T >$ LCST are known in the literature.[19,20] But to our knowledge, this is the first study exploring a reversible photo-cross-linking reaction for photoresponsive nanogels, aiming to disclose a new optical control mechanism for hydrogels' volume change.

2. Experimental Section

1. Materials. All chemicals were purchased from Aldrich. 2-(2-Methoxyethoxy)ethyl methacrylate (MEOMA) was passed through a basic aluminum oxide column prior to use. Poly (ethylene oxide) (PEO) macroinitiator was prepared by reacting PEO monomethyl ether (M_n = 5000 g/mol) and 2-bromoisobutyryl bromide using a literature method.[21] 4-Methyl-[7-(methacryloyl)oxyethyloxy]coumarin (coumarin methacrylate, CMA) was synthesized using the method previously reported.[16] Dipyridamole (DIP, >98%), Nile Red (NR), *N*,*N*,*N*′,*N*′,*N*″-pentamethyldiethylenetriamine (PMDETA, 99%), anhydride anisole (99%), and copper chloride (Cu(I)Cl, 99%) were used without further purification.

2. Synthesis of Block Copolymers. Using the same macroinitiator of PEO_{112}-Br, diblock copolymers with various P(MEOMA-*co*-CMA) blocks, differing in the absolute molecular weight and the content of photo-cross-linkable coumarin groups, were synthesized by atom transfer radical polymerization (ATRP) (Scheme 1). Using the sample PEO_{112}-*b*-P($MEOMA_{90}$-*co*-CMA_{12}) as an example, a detailed synthetic procedure is as follows. CuCl(I) (12 mg, 0.12 mmol), PEO_{112}-Br (200 mg, 0.04 mmol), PMDETA (54 μL, 0.24 mmol), MEOMA (1.13 g, 6 mmol), and CMA (162 mg, 0.6 mmol) were dissolved in 4 mL of anisole in a 10 mL flask under a N_2 atmosphere. The reaction mixture was degassed by three freeze−pump−thaw cycles and then filled with N_2. The flask was placed in a preheated oil bath at 60 °C for 60 min. After the polymerization, the reaction mixture was cooled to room temperature and diluted with THF. The catalyst was removed by passing the mixture through a neutral alumina column. The solution was then concentrated and precipitated twice in a mixture of pentane and diethyl ether (1:1, v/v), followed by precipitation in pentane alone for two more times. The block copolymer was filtered and dried at 40 °C for 24 h. According to GPC measurements (PS standards), the polymer has a M_n of 28 700 g/mol and a polydispersity index (M_w/M_n) of 1.08. From the ^{1}H NMR spectrum, comparing the integrals of the resonance peaks of $-OCH_2CH_2-$ of PEO and PMEOMA (3.65 ppm), $-O-CH_3$ of PMEOMA (3.39 ppm) and $-CH_3$ of CMA (2.42 ppm) led to the estimation of 90 units of MEOMA and 12 units of CMA, corresponding to a NMR-based M_n of 25 380 g/mol.

3. Characterizations. Gel permeation chromatography (GPC) measurements were performed on a Waters system equipped with a refractive index detector (RI 410) and a photodiode array detector (PDA 996). THF was used as the eluent at an elution

Table 1. Characteristics of Synthesized Block Copolymers

sample	$M_{n,GPC}$ (g/mol)[a]	$M_{n,NMR}$ (g/mol)[b]	PDI	n_{MEOMA}:n_{CMA}[c]	$LCST_{DLS}$ (°C)[d]	$LCST_F$ (°C)[e]
PEO_{112}-*b*-$PMEOMA_{112}$	38 800	26 000	1.10	1:0	31	30
PEO_{112}-*b*-$PMEOMA_{273}$	62 200	56 300	1.12	1:0	28	27
PEO_{112}-*b*-P($MEOMA_{83}$-*co*-CMA_6)	29 300	22 230	1.07	1:0.067	25	23
PEO_{112}-*b*-P($MEOMA_{90}$-*co*-CMA_{12})	28 700	25 380	1.08	1:0.134	17	16
PEO_{112}-*b*-P($MEOMA_{188}$-*co*-CMA_{14})	44 900	41 200	1.07	1:0.075	21	19
PEO_{112}-*b*-P($MEOMA_{175}$-*co*-CMA_{19})	49 800	43 660	1.10	1:0.110	17	12

[a] Determined by GPC using polystyrene for calibration. [b] Calculated from block copolymer composition as determined by ^{1}H NMR spectroscopy. [c] Calculated from ^{1}H NMR spectra. [d] Measured as the onset of the abrupt increase in scattering intensity. [e] Determined as the onset of the abrupt increase in fluorescence emission of Nile Red.

rate of 1 mL min^{-1}, while polystyrene standards were used for calibration. ^{1}H NMR spectra were obtained with a Bruker spectrometer (300 MHz, AC 300). For the variable-temperature measurements, the spectra were recorded after the solution was held at a given temperature for 10 min for equilibrium. Dynamic light scattering (DLS) experiments were carried out on a Brookhaven goniometer (BI-200) equipped with a highly sensitive avalanche photodiode detector (Brookhaven, BI-APD), a digital correlator (Brookhaven, TurboCorr) that calculates the photon intensity autocorrelation function $g^2(t)$, a helium−neon laser (wavelength λ = 632.8 nm), and a thermostat sample holder. The hydrodynamic diameter (D_H) of micellar aggregates was obtained by cumulants and CONTIN analyses, and the light scattering intensity was measured at 90°. All initial solutions were filtered with a 200 nm pore filter and, before the DLS measurement at each temperature, the solution was equilibrated for 10 min. Each DLS measurement was performed three times to calculate the average hydrodynamic diameter. The photo-cross-linking of coumarin side groups was obtained by using a UV−vis spot curing system (Novacure) with a 320−500 nm filter generating UV light at λ > 310 nm (intensity at 320 nm is ~35 mW cm^{-2}). For the photocleavage of cyclobutane rings (photo-de-cross-linking), a UV-C Air sterilizer lamp (1.25 W) peaked at λ = 254 nm was used at a distance of 5 cm to the nanogel solution. Fluorescence emission spectra were recorded on a fluorescence spectrophotometer (Varian Cary Eclipse) equipped with thermostat sample holder (Varian SPVF), while UV−vis spectra were taken using a spectrophotometer (Varian 50 Bio). The dimerization degree of coumarin was calculated from the decrease in absorbance of the peak around 320 nm. Observation of photo-cross-linked and photo-de-cross-linked nanogel particles was made on a Nanoscope 3A atomic force microscope (AFM) in tapping mode. The dry samples were prepared by directly dipping a clean mica substrate in the solution, followed by drying at room temperature. Solution-cast samples on silicon wafers were also examined on a Hitachi S-4700 field-emission-gun scanning electron microscope (SEM) operating at 3 kV.

To investigate the effect of photocontrollable cross-linking degree on the release of guest molecules from the nanogel, DIP and NR were utilized. For the loading of DIP, 4 mL of a PEO_{112}-*b*-P($MEOMA_{83}$-CMA_6) solution (2 mg mL^{-1}) was first heated to 40 °C to form the micelles; after 10 min for equilibrium, 100 μL of a DIP ethanol solution (20 mg mL^{-1}) was then added slowly (25 μL per 30 s). The mixture was stirred at 40 °C for 12 h for the encapsulation of DIP. Ethanol was removed by evaporation in a vacuum oven, before more water was added and insolubly nonencapsulated DIP removed by microfiltration (200 nm pore filter). In the case of NR, it was loaded in the nanogel by mixing 10 μL of an acetone solution of the dye (0.06 mg mL^{-1}) with 2 mL of the micellar solution (2 mg mL^{-1}) at 40 °C. As will be shown later, the release of loaded dyes from the nanogel at 10 °C could be monitored by measuring changes in either fluorescence emission or absorption of the dyes as a function of time. Moreover, the change in fluorescence emission of NR (excitation wavelength: 550 nm) as a function of temperature, associated with the solubilization of NR upon micelle formation, was used to determine the LCST of block copolymers. In this case, emission spectra were recorded at various temperatures (solution equilibrated at each temperature for 5 min).

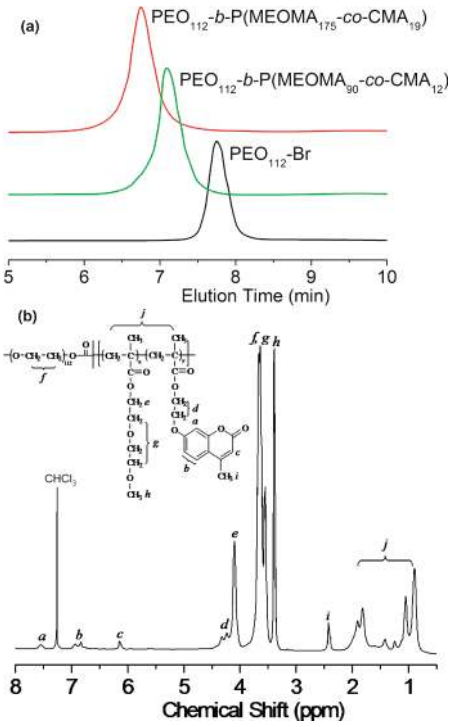

Figure 2. (a) GPC traces of two coumarin-containing block copolymers and the macroinitiator. (b) ^{1}H NMR spectrum (in $CDCl_3$) of the block copolymer of PEO_{112}-*b*-P($MEOMA_{90}$-*co*-CMA_{12}).

3. Results and Discussion

1. Synthesis, Characterization, and Thermoresponsive Behavior. Diblock copolymers of PEO-*b*-P(MEOMA-*co*-CMA), being both thermosensitive and photosensitive, were prepared by ATRP using a PEO_{112}-Br macroinitiator. The polymerizations were carried out with the Cu(I)Cl/PMDETA catalytic system in anisole at 60 °C. By adjusting the mole ratio of the two monomers of MEOMA and CMA, a series of block copolymers with various molecular weights and compositions were obtained, as shown in Table 1. For comparison, samples without photoactive CMA units were also prepared. The block copolymers with CMA were precipitated twice in pentane and diethyl ether (1:1, v/v) to remove unreacted CMA monomer. The precipitation and filtration should be conducted at very low temperature with dry ice to obtain powder samples. Examples of GPC curves are shown in Figure 2a, indicating the controlled growth of the second random copolymer block of P(MEOMA-*co*-CMA), with a low polydispersity index of ~1.10. Figure 2b shows the ^{1}H NMR spectrum in $CDCl_3$ of one sample (PEO_{112}-*b*-P($MEOMA_{90}$-*co*-CMA_{12}). Knowing the molecular weight of the

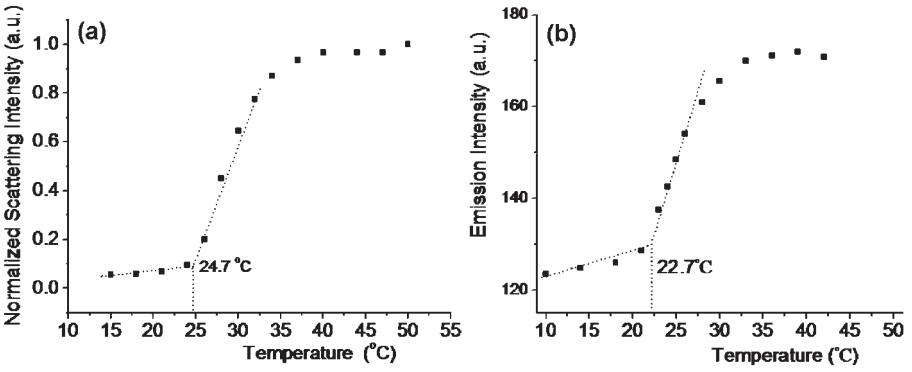

Figure 3. Determination of the lower critical solution temperature (LCST) for the block copolymer PEO_{112}-*b*-P($MEOMA_{83}$-*co*-CMA_6) in an aqueous solution (2 mg mL^{-1}) using various-temperature dynamic light scattering (DLS) (a) and fluorescence emission of Nile Red (b).

PEO block, the relative amount of MEOMA could readily be calculated by comparing the integrals of the resonance peaks *f*, *g* (from PEO and the side chain of MEOMA), and *h* (from the methyl group in side chain of MEOMA). The mole ratio of CMA as compared to MEOMA in the random copolymer block was determined from the integrals of the peak *i* (from the methyl group in side chain of CMA) and the peak *h*. The NMR analysis results are summarized in Table 1.

It is known that the homopolymer PMEOMA has a LCST around 25 °C, and the block copolymer PEO-*b*-PMEOMA could form micelles with PMEOMA core at $T >$ LCST.[22] With the incorporation of CMA comonomer units into the thermoresponsive PMEOMA, it was expected that the LCST of the new diblock copolymer might be affected, but the formation of micelles, which is necessary for the preparation of our photoresponsive nanogels, would be preserved. We thus investigated the thermally induced micellization behavior of the block copolymers by means of DLS and fluorescence spectroscopy. The results in Figure 3, obtained with the sample of PEO_{112}-*b*-P($MEOMA_{83}$-*co*-CMA_6), clearly show the micellization related to LCST of the P(MEOMA-*co*-CMA) block. With DLS, the scattering intensity of an aqueous solution of the block copolymer (2 mg mL^{-1}) was recorded as a function of temperature (Figure 3a). The abrupt increase at ~25 °C indicates the transformation from dissolved polymer chains to micelles when the P(MEOMA-*co*-CMA) block undergoes the hydration to dehydration transition and becomes insoluble in water. The change of scattering intensity was accompanied by an increase in hydrodynamic diameter (D_H) (data not shown), while the LCST determined as the onset of the abrupt increase is about 25 °C. Using an aqueous solution of the polymer (2 mg mL^{-1}) equilibrated with NR, the fluorescence emission spectral change of NR upon heating (spectra in Supporting Information) also allowed the LCST to be determined. An increase in emission intensity and a blue shift of the maximum emission wavelength of NR were observed with increasing the temperature, indicating that NR molecules were located in an increasingly hydrophobic (dehydrated) environment.[22−24] From the plot of emission intensity vs temperature in Figure 3b, the hydration to dehydration transition is clear; the LCST thus determined is about 23 °C, slightly lower than that from DLS. All the results confirmed the formation of micelles of the diblock copolymer at $T >$ LCST. The values of LCST as measured by the two techniques are given in Table 1. With a similar molecular weight for the P(MEOMA-*co*-CMA) block, a higher content of the CMA comonomer units results in a lower LCST due to the hydrophobicity of the coumarin moiety. As compared to PEO-*b*-PMEOMA, the presence of coumarin units in PEO-*b*-P(MEOMA-*co*-CMA) reduces markedly the LCST. We note that two independent series of DLS measurements were performed and yielded almost identical LCST values (within 1 °C), thus confirming the good reproducibility of the results.

2. Preparation of Nanogels with Phototunable Cross-Linking Density. As mentioned above, coumarin could undergo a photodimerization reaction under $\lambda > 310$ nm and the reverse photocleavage reaction under $\lambda < 260$ nm UV light. This may allow a polymer containing pendant coumarin groups to be reversibly cross-linked and de-cross-linked using two different wavelengths. Our interest in the present study is to make use of this appealing property to construct a general strategy for preparation of photoresponsive nanogels via block copolymer self-assembly in aqueous solution (Figure 1). With PEO-*b*-P(MEOMA-*co*-CMA) dissolved in water, the chains aggregate on heating to $T >$ LCST to form micelles with a core of the coumarin-containing polymer. Upon exposure of the micelles to $\lambda > 310$ nm light, they can be cross-linked, while by bringing the solution temperature back to $T <$ LCST, the cross-linked micelles become nanogels since they are nanoparticles of a cross-linked water-soluble polymer.

Using an aqueous solution of PEO_{112}-*b*-P($MEOMA_{175}$-*co*-CMA_{19}) (0.2 mg mL^{-1}), we first investigated the reversibility of the photo-cross-linking reaction in the micellar aggregates and its effect on the obtained nanogels. Figure 4a shows the UV−vis spectral change of the micellar solution at 40 °C (above the LCST) upon irradiation of $\lambda > 310$ nm UV light. The decrease in the absorption of coumarin groups, peaked at ~320 nm, over irradiation time indicates the occurrence of dimerization and thus the cross-linking of the micelles. From the spectra, the dimerization degree, defined as $(1 - A_t/A_0)$ with A_0 and A_t being the initial absorbance at 320 nm and the absorbance after an irradiation time *t*, respectively, could be calculated; the result given in the inset shows the kinetic process and that the dimerization degree reaches a plateau value of ~85% after 200 s. As the resulting dimer form with cyclobutane ring (Figure 1) absorbs light at $\lambda < 260$ nm, when light applied to the micellar solution was changed to $\lambda < 260$ nm, the absorbance at 320 nm started to recover as a result of the reverse photocleavage reaction bringing back coumarin side groups, as shown in Figure 4b. The reversibility of the photoreaction with micelles at 40 °C was confirmed by five consecutive cycles of photodimerization and photocleavage. The result in Figure 4c shows that the dimerization degree could be switched between ~85% and 25% by alternating UV exposure at $\lambda > 310$ nm and $\lambda < 260$ nm. Considering the moderate concentration of CMA units in the P(MEOMA-*co*-CMA) block (from ~7 to 13 mol %), it is reasonable to

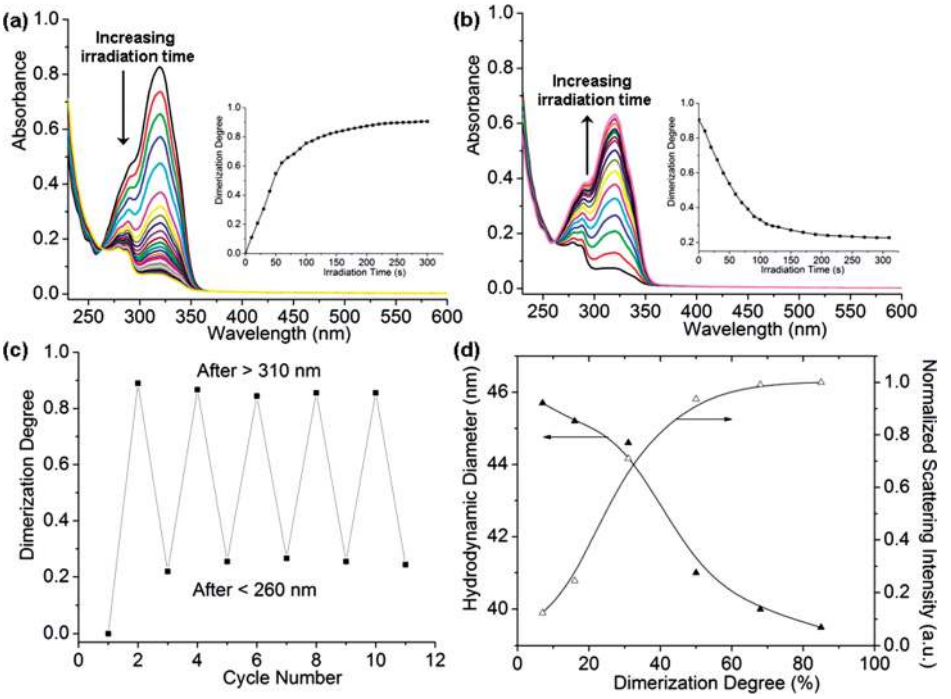

Figure 4. UV−vis and DLS results obtained with an aqueous solution of PEO_{112}-*b*-P($MEOMA_{175}$-*co*-CMA_{19}) showing the photocontrol of cross-linking degree in preparing the nanogel: (a) decrease of the absorbance at 320 nm upon illumination at $\lambda > 310$ nm (with 10 s intervals) indicating the dimerization of coumarin groups in micelles at $T >$ LCST (40 °C), with in the inset the plot of dimerization degree vs irradiation time; (b) increase of the absorbance at 320 nm when exposed to $\lambda < 260$ nm light (with 10 s intervals for the first 130 and 20 s for the rest) indicating the reverse photoreaction of cyclobutane cleavage, with in the inset the plot of the dimerization degree vs irradiation time; (c) reversible change in the dimerization degree of micelles upon alternating UV illumination at $\lambda > 310$ nm for dimerization (5 min exposure) and at $\lambda < 260$ nm for cleavage (5 min); and (d) dependence of the average hydrodynamic diameter of nanogel particles at $T <$ LCST (10 °C) on the dimerization degree and the corresponding change in the scattering intensity measured at 90°.

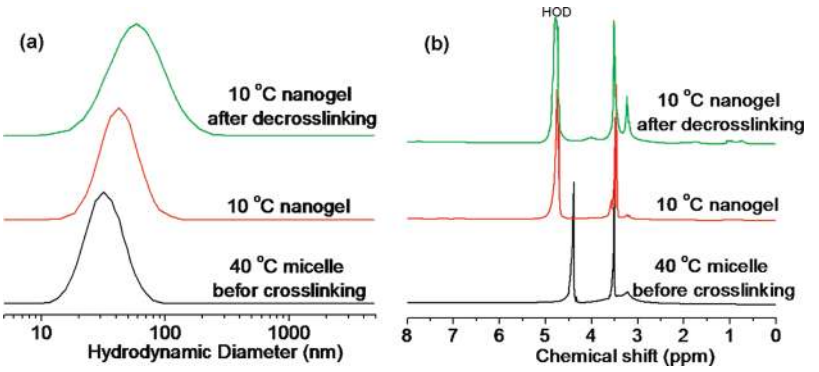

Figure 5. (a) Size distribution and (b) ^{1}H NMR spectra (in D_2O) for micelles at $T >$ LCST (40 °C), nanogel particles at $T <$ LCST (10 °C), and de-cross-linked nanogel, obtained with PEO_{112}-*b*-P($MEOMA_{83}$-*co*-CMA_6) (2 mg mL^{-1}).

assume that most dimerization occurs between coumarin groups on different polymer chains so that the dimerization degree is indicative of the cross-linking density. This was confirmed by the result in Figure 4d. In this experiment, micelles formed at 40 °C were subjected to $\lambda > 310$ nm irradiation for various degrees of photodimerization of coumarin groups, and the resulting nanogels at 10 °C were characterized by DLS (a higher polymer concentration of 2 mg mL^{-1} was used for better DLS measurements). As can be seen, the average hydrodynamic diameter (D_H) of the nanogel is directly correlated to the dimerization degree. Since highly cross-linked nanogel absorbs less water, it swells less, resulting in a smaller size. The result shows that to produce nanogels swellable to various extents, the cross-linking density could easily be controlled by the dimerization degree in the micellar state. Figure 4d also shows that as the nanogel swells more with reducing the cross-linking density (D_H increases), the scattering intensity decreases. This should be caused by, on the one hand, a reduced contrast of the refractive index between highly hydrated nanogel and water and, on the other hand, the dissolution of some polymer chains in the solution. It is noted that the increase in scattering intensity as the nanogel particles deswell is consistent with what was observed with thermally induced volume transition of PNIPAM nanogels.[2]

3. Photoresponsive Behavior of Nanogels. The dependence of swelling on cross-linking degree suggests that such nanogels could respond to light exposure that changes the cross-links. We investigated the photoresponsive behavior of the nanogel in aqueous solution. Figure 5 shows the results of DLS and ^{1}H NMR (in D_2O) obtained with PEO_{112}-*b*-P($MEOMA_{83}$-*co*-CMA_6) (2 mg mL^{-1}). At 40 °C, the DLS measurement shows micelles having an average D_H of 35 nm, while in the ^{1}H spectrum the resonance signals

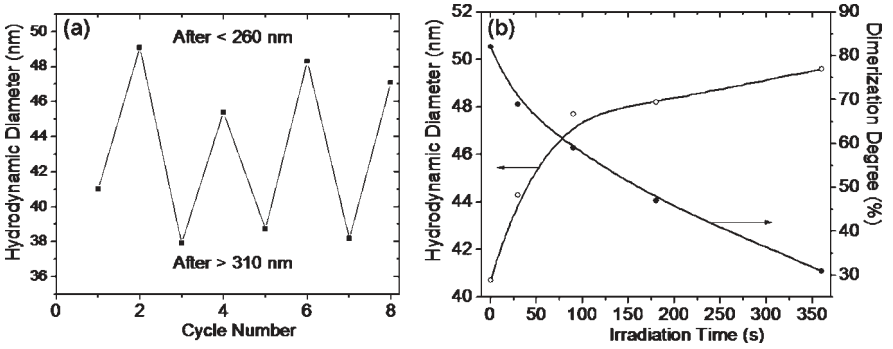

Figure 6. DLS results obtained with PEO_{112}-*b*-P($MEOMA_{83}$-*co*-CMA_6) (2 mg mL^{-1}) showing the photochangeable volume of nanogel particles: (a) reversible change in hydrodynamic diameter at 10 °C upon alternating photo-de-cross-linking at $\lambda < 260$ nm (8 min exposure) and photo-cross-linking at $\lambda > 310$ nm (12 min), with the solution heated to 40 °C before cooling back to 10 °C; (b) increase in hydrodynamic diameter of nanogel particles and the corresponding decrease in dimerization degree of coumarin groups vs irradiation time upon $\lambda < 260$ nm exposure.

of the micelle core-forming P(MEOMA-*co*-CMA) block can hardly be noticed due to the compact aggregation of the chains. After photo-cross-linking to a dimerization degree of about 85% using $\lambda > 310$ nm light, and with the solution cooled to 10 °C, the nanogel swells in water as the DLS indicates a D_H of ~40 nm. However, the ^{1}H NMR spectrum displays little change except the temperature change induced shift of the solvent peak (residual HOD),[19] suggesting that even in the hydrated state the P(MEOMA-*co*-CMA) chains of the highly cross-linked nanogel were still densely packed. Indeed, by exposing the nanogel to UV light of $\lambda < 260$ nm, which reduces the dimerization degree to ~25%, the volume of the nanogel increases significantly as the D_H goes up to 49 nm. Swollen nanogel particles also display a larger dispersity index (from 0.09 before to 0.3 after the de-cross-linking). The highly swollen state is also revealed by the ^{1}H NMR spectrum on which the signals of the solvated P(MEOMA-*co*-CMA) chains at 4.0 and 3.3 ppm reappear. These results clearly show the photoinduced volume increase of the nanogel based on the photocontrollable cross-linking density.

The photoinduced volume increase of the nanogel due to the transition from a highly to a lightly cross-linked state could be repeated many times. However, the initial highly cross-linked state could not be recovered by direct photo-cross-linking of the swollen nanogel. Instead, it could be reestablished by heating the solution to $T >$ LCST (40 °C) for volume contraction, followed by photo-cross-linking and cooling of the solution to $T <$ LCST (10 °C). Again with PEO_{112}-*b*-P($MEOMA_{83}$-*co*-CMA_6), Figure 6a shows the results of four cycles of volume increase induced by $\lambda <$ 260 nm light (8 min, solution volume 2 mL, dimerization down to ~25%) and volume decrease obtained by the combined use of thermal effect and $\lambda > 310$ nm light (12 min, dimerization up to ~85%). The average photoinduced increase in D_H due to de-cross-linking is from about 39 to 48 nm; that is about 23% increase in hydrodynamic diameter, corresponding to a volume increase of ~90% for the nanogel. In one cycle of those measurements, the decrease in the dimerization degree upon irradiation with $\lambda < 260$ nm light and the corresponding equilibrium D_H (10 min at 10 °C after each exposure) were monitored at various irradiation times; the result is given in Figure 6b. As expected, the degree of photoinduced swelling of the nanogel is dependent upon the extent of de-cross-linking. But interestingly, the result shows that most of the volume increase upon irradiation was achieved when the dimerization degree was reduced from ~82% to ~60%, while the further de-cross-linking resulted in small increase of swelling. Under the used conditions, it took about 100 s to get the dimerization degree down to ~60%. To obtain some information on the kinetics of the photoinduced volume increase, we performed the following experiment. Immediately after 2 min of irradiation with $\lambda < 260$ nm light, the scattering intensity from the solution was measured over time. Only a small increase within the first 30 s was observed after turning off the light before the scattering intensity became constant. (The small increase is probably caused by a re-equilibration due to a small cooling of the solution upon removal of light irradiation.) Considering the fact that if the nanogel volume increase took some time to develop after the 2 min irradiation, a decrease in the scattering intensity would be observed (Figure 4c), this result suggests that the nanogel swelling was essentially completed during the course of the 2 min de-cross-linking. In other words, this photoinduced volume transition of the nanogel is fast.

All samples of PEO-*b*-P(MEOMA-*co*-CMA) in Table 1 were investigated under the same conditions of nanogel preparation and experiments for photoresponsive behaviors as described above. The results are summarized in Table 2 showing, in particular, their average photoinduced volume transition, i.e., the increase in D_H upon de-cross-linking and the corresponding volume variation. Both the molecular weight of the P(MEOMA-*co*-CMA) block and the content of the coumarin comonomer appear to affect the photoinduced volume increase of the nanogel. A greater effect was observed for nanogels prepared with block copolymer samples having a lower molecular weight of the P(MEOMA-*co*-CMA) block. It seems that a smaller core of cross-linked P(MEOMA-*co*-CMA) reacts more strongly to the photocontrolled cross-linking density. Comparing the two samples with a shorter P(MEOMA-*co*-CMA) block, at the same dimerization degree of ~85%, the higher concentration of coumarin side groups gave rise to less swollen nanogel at 10 °C due to a greater cross-linking density. However, the photo-de-cross-linking resulted in a similar volume increase (~90%) of the nanogel. For the two samples with a longer P(MEOMA-*co*-CMA) block, the difference in the concentration of coumarin groups showed little effect on the photoinduced volume change of the nanogels. Another point is worth being made. Considering that the un-cross-linked PEO corona should not contribute to the observed increase in the hydrodynamic diameter upon photo-de-cross-linking, more important photoinduced volume transition could be obtained with nanogel particles with shell and core both cross-linked.

Cross-linked and de-cross-linked nanogel particles (~85 and 25% dimerization degree, respectively) in the dried state could be observed on AFM and SEM, as shown in Figure 7 with images obtained using PEO_{112}-*b*-P($MEOMA_{83}$-*co*-CMA_6). De-cross-linked particles appear slightly bigger

Table 2. Average Hydrodynamic Diameters (in nm) of Micelles (at 40 °C) and Nanogel Particles (at 10 °C)[a]

sample	micelle before cross-linking	micelle after cross-linking	nanogel	nanogel after de-cross-linking	nanogel volume change after de-cross-linking (V/V_0)[b]
PEO_{112}-*b*-P($MEOMA_{83}$-*co*-CMA_6)	36.3 ± 0.9	31.2 ± 2.7	39.1 ± 1.9	48.3 ± 1.4	1.9
PEO_{112}-*b*-P($MEOMA_{90}$-*co*-CMA_{12})	31.5 ± 1.1	29.9 ± 0.8	35.8 ± 2.1	44.0 ± 2.3	1.9
PEO_{112}-*b*-P($MEOMA_{188}$-*co*-CMA_{14})	36.6 ± 0.9	31.7 ± 1.1	39.1 ± 1.1	46.3 ± 1.9	1.7
PEO_{112}-*b*-P($MEOMA_{175}$-*co*-CMA_{19})	36.8 ± 1.5	34.9 ± 0.8	39.2 ± 0.7	44.2 ± 0.9	1.4

[a] Reported data are the average values with standard deviations obtained from at least three measurements. [b] V_0 and V are the average hydrodynamic volume of the nanogel particle before and after photo-de-cross-linking, respectively.

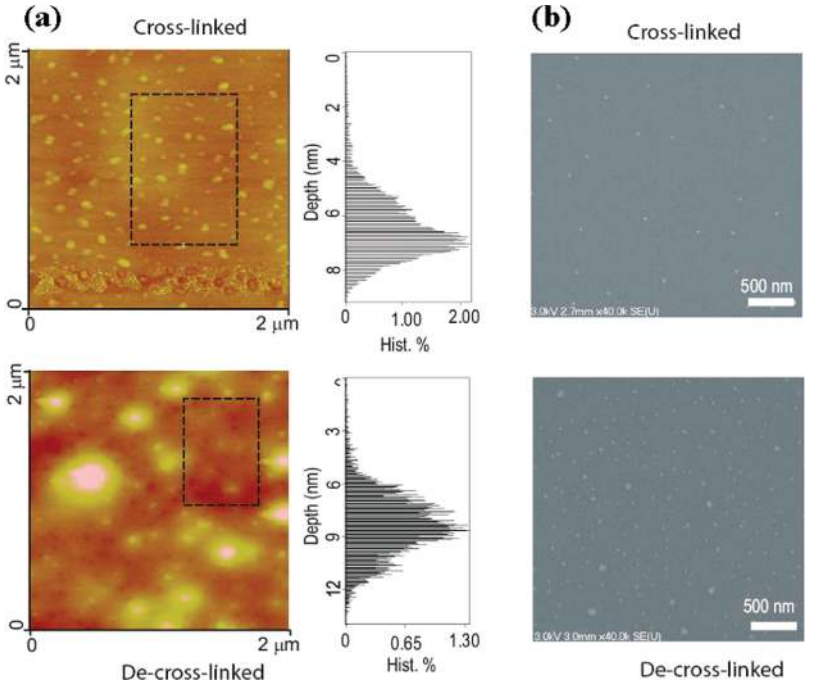

Figure 7. Cross-linked and de-cross-linked nanogel particles viewed at the dry state: (a) AFM topological images with depth histograms for marked region; (b) SEM images.

and have a larger size distribution than cross-linked particles, especially with some larger aggregates observable on the AFM image. But most particles have similar sizes of around 30 nm. This is understandable because the photoinduced swelling of nanogel particles in solution comes from a larger amount of absorbed water; as water is evaporated, the particles would shrink. The depth histograms of AFM covering the marked areas for the two samples (large aggregates avoided) indicate that de-cross-linked particles also have a larger average height (~9 nm) than that of cross-linked ones (~7 nm). The fact that in both cases the heights of the particles are much smaller than their sizes in the substrate plane indicates that they are flattened in the course of water evaporation.

4. Photocontrolled Release from Nanogels. In addition to the aforementioned valve in a microfluidic device,[15] another possible application of the photocontrollable volume change of nanogel particles is to control the release rate of loaded guest molecules. Using the sample of PEO_{112}-*b*-P($MEOMA_{83}$-*co*-CMA_6), we performed a number of experiments to investigate this possibility. The first experiment was designed to observe the effect of photoinduced swelling of nanogel particles on the release rate in situ. Dipyridamole (DIP) was first loaded in micelles at 40 °C;[25] then half of the micellar solution was exposed to $\lambda > 310$ nm UV light for full cross-linking (dimerization degree ~ 85%), while the other half was left un-cross-linked. For the measurements, 0.3 mL of each solution was placed in a dialysis cap immersed in 3 mL of water/dioxane (2:1, v/v) thermostated at 10 °C and

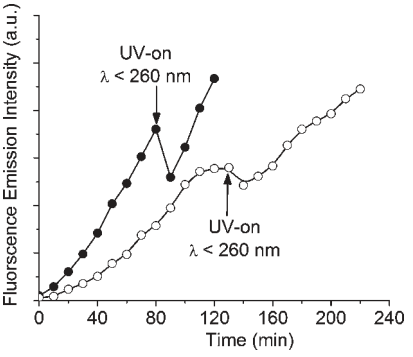

Figure 8. Fluorescence emission intensity of dipyridamole at 486 nm (λ_{ex} = 415 nm) vs time for dye-loaded non-cross-linked micelles (●) and cross-linked nanogel (○) at 10 °C in a dialysis cap immersed in water/diaoxane (2:1, v/v), photo-de-cross-linking of the nanogel being obtained by $\lambda < 260$ nm exposure for 3 min.

filled in a UV cell.[26] The release of DIP into the solution by diffusing through the membrane was monitored by measuring the fluorescence emission of the dye at 486 nm (excitation at 415 nm) at time intervals of 10 min. Figure 8 shows the plots of fluorescence emission intensity vs time. It is evident that the release of DIP from un-cross-linked micelles was much faster than from the cross-linked nanogel. With the micelles, no slowdown of the release was observed after 80 min when, as a control test, the solution was exposed to $\lambda < 260$ nm UV for 3 min; the following measurement showed a decrease of the fluorescence intensity likely due

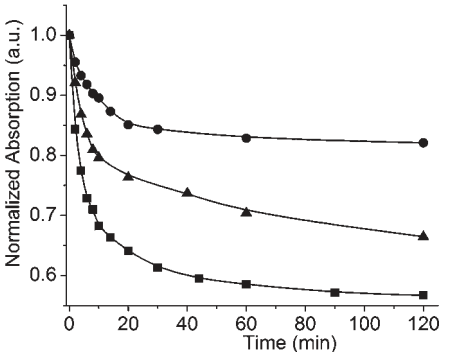

Figure 9. Normalized absorbance of Nile Red at 550 nm vs time for dye-loaded non-cross-linked micelles (■) and nanogels with 20% (▲) and 60% (●) dimerization degree at 10 °C in aqueous solution.

to some photobleaching effect. But the release then resumed with the same rate. In the case of nanogel, the release was much slowed down from 100 min, with the fluorescence intensity reaching a plateau level. However, after a 3 min exposure to $\lambda < 260$ nm light for nanogel de-cross-linking, the release rate increased sharply following a slight irradiation-induced decrease of fluorescence intensity. This result shows clearly that the swelling of nanogel particles in solution as a result of photoinduced de-cross-linking can speed up the release of loaded molecules.

Another way to control the release rate would be to optically tune the prefixed cross-linking density of the nanogel. To investigate this possibility, Nile Red (NR) was first loaded in micelles at 40 °C, and then two aliquots of the solution were photo-cross-linked to different degrees with 20 and 60% dimerization of coumarin groups, respectively, and compared with un-cross-linked micelles. For this experiment, the three solutions were brought to 10 °C to allow the swelling of nanogel particles and the release of guest molecules. When released into an aqueous medium, NR molecules became insoluble, resulting in a decrease in its absorption at 550 nm, and the absorbance could be monitored once the solutions were cooled to 10 °C. Figure 9 shows the plots of normalized absorbance A/A_0 vs time for the two nanogels and the non-cross-linked micelles, A_0 being the absorbance at 40 °C before the release. It can be seen that the dissolution of non-cross-linked chains results in the fastest release of loaded dye molecules, while the release is increasingly slower with increasing the cross-linking density due to smaller swelling of the nanogel particles.

4. Conclusions

We presented a new and general strategy for preparing photoresponsive nanogels. It is based on the use of photocontrollable cross-linking density to determine the swelling of nanogel particles in aqueous solution. This control mechanism allows the volume of nanogel particles to be changed gradually by illumination, which differs from the approaches based on a photothermal effect or photoinduced change in hydrophilicity. For proof-of-principle, diblock copolymers of PEO-*b*-P(MEOMA-*co*-CMA) bearing coumarin side groups were synthesized. Water-soluble nanoparticles were obtained by first forming micelles at $T >$ LCST of P(MEOMA-*co*-CMA), then cross-linking micelles through dimerization of coumarin groups under $\lambda > 310$ nm UV light, and finally bringing the solution to $T <$ LCST. Upon exposure to $\lambda < 260$ nm UV light, the reverse photocleavage of cyclobutane bridges could reduce the cross-linking density and lead to an increase in volume of nanogel particles by ~90%. The initial hydrogel could be recovered by photo-cross-linking at $T >$ LCST and the photoinduced volume transition could be repeated. Moreover, we showed the possibility of using this type of photoresponsive nanogels to optically control the release of loaded quest molecules. This can be achieved either by direct photo-de-cross-linking of nanogel particles in solution or by optically tuning the cross-linking degree in preparing the nanogel.

Acknowledgment. We acknowledge financial support from the Natural Sciences and Engineering Research Council of Canada (NSERC) and le Fonds québécois de la recherche sur la nature et les technologies of Québec (FQRNT). Y.Z. is a member of the FQRNT-funded Center for Self-Assembled Chemical Structures (CSACS).

Supporting Information Available: Absorption and fluorescence emission spectra of Nile Red and dipyridamole loaded in nanogel particles. This material is available free of charge via the Internet at http://pubs.acs.org.

References and Notes

(1) Pelton, P. *Adv. Colloid Interface Sci.* **2000**, *85*, 1.
(2) Wang, J.; Gan, D.; Lyon, L. A.; El-Sayed, M. *Macromolecules* **2001**, *123*, 11248.
(3) Xia, X.; Tang, S.; Lu, X.; Hu, Z. *Macromolecules* **2003**, *36*, 3695.
(4) Holtz, J. H.; Asher, S. A. *Nature (London)* **1997**, *389*, 829.
(5) Peng, S.; Wu, C. *Macromolecules* **2001**, *34*, 568.
(6) Jones, C. D.; Lyon, L. A. *J. Am. Chem. Soc.* **2003**, *125*, 460.
(7) Gorelikov, I.; Field, L. M.; Kumacheva, E. *J. Am. Chem. Soc.* **2004**, *126*, 15935.
(8) Zhu, M.-Q.; Zhu, L.; Han, J.; Wu, W.; Hurst, J. K.; Li, A. D. Q. *J. Am. Chem. Soc.* **2006**, *128*, 4303.
(9) Hirakura, T.; Nomura, Y.; Aoyama, Y.; Akiyoshi, K. *Biomacromolecules* **2004**, *5*, 1804.
(10) Garcia, A.; Marquez, M.; Cai, T.; Rosario, R.; Hu, Z.; Gust, D.; Hayes, M.; Vail, S. A.; Park, C.-D. *Langmuir* **2007**, *23*, 224.
(11) Irie, M.; Kungwatchakun, D. *Macromolecules* **1986**, *19*, 2476.
(12) Suzuki, A.; Tanaka, T. *Nature (London)* **1990**, *346*, 345.
(13) Sershen, S. R.; Westcott, S. L.; Halas, N. J.; West, J. L. *J. Biomed. Mater. Res.* **2000**, *51*, 293.
(14) Sumaru, K.; Ohi, K.; Takagi, T.; Kanamori, T.; Shinbo, T. *Langmuir* **2006**, *22*, 4353.
(15) Sershen, S. R.; Mensing, G. A.; Ng, M.; Halas, N. J.; Beebe, D. J.; West, J. L. *Adv. Mater.* **2005**, *17*, 1366.
(16) Jiang, J.; Qi, B.; Lepage, M.; Zhao, Y. *Macromolecules* **2007**, *40*, 790.
(17) Babin, J.; Lepage, M.; Zhao, Y. *Macromolecules* **2008**, *41*, 1246.
(18) Trenor, S. R.; Shultz, A. R.; Love, B. J.; Long, T. E. *Chem. Rev.* **2004**, *104*, 3059.
(19) Kuckling, D.; Vo, C. D.; Adler, H.-J. P.; Volkel, A.; Colfen, H. *Macromolecules* **2006**, *39*, 1585.
(20) Zhang, J.; Jiang, X.; Zhang, Y.; Li, Y.; Liu, S. *Macromolecules* **2007**, *40*, 9125.
(21) Tian, Y.; Watanabe, K.; Kong, X.; Abe, J.; Iyoda, T. *Macromoelcules* **2002**, *35*, 3739.
(22) Jiang, X.; Zhao, B. *Macromoelcules* **2008**, *41*, 9366.
(23) Goodwin, A. P.; Mynar, J. L.; Ma, Y.; Fleming, G. R.; Frechet, J. M. J. *J. Am. Chem. Soc.* **2005**, *127*, 9952.
(24) Jiang, J.; Tong, X.; Zhao, Y. *J. Am. Chem. Soc.* **2005**, *127*, 8290.
(25) Li, Y.; Lokitz, B. S.; Arms, S. P.; McCormick, C. L. *Macromoelcules* **2006**, *40*, 2726.
(26) Babin, J.; Pelletier, M.; Lepage, M.; Allard, J. F.; Morris, D.; Zhao, Y. *Angew. Chem., Int. Ed.* **2009**, *48*, 3329.